Origin of Diastereoselectivity in the Synthesis of Chiral Bicyclic Lactams: π-Facial Selective Attack of Singlet Oxygen Induced by Hindered Internal Rotation

Saron Catak,[†] Hasan Celik,[†] Ayhan S. Demir,[‡] and Viktorya Aviyente*[,†]

Departments of Chemistry, Bogazici University, 34342 Bebek, Istanbul, Turkey, and Middle East Technical University, 06531 Ankara, Turkey

Received: February 27, 2007; In Final Form: April 23, 2007

Previously reported experimental results indicate that photooxygenation of homochiral *N*-(hydroxyalkyl)-2-methylpyrroles with singlet oxygen yields trans—rather than cis-bicyclic lactams as the major product. In this study, the origin of selectivity in this reaction has been investigated with computational methods. Relative stabilities of homochiral *N*-(hydroxyalkyl)-2-methylpyrrole conformers and their effect on π-facial selectivity of $^1O_2$ were extensively studied. Stepwise and concerted reaction mechanisms, starting from the endoperoxide intermediates, were proposed and modeled in vacuum using the UB3LYP method with the 6-31+G** basis set. Solvent calculations were carried out in CH_2Cl_2, by means of the integral equation formalism-polarizable continuum model (IEF-PCM) at the UB3LYP/6-31+G** level of theory. Free energies of activation leading to both diastereomers were analyzed in an effort to explain the stereoselectivity and product distribution. Steric interactions among the pyrrole substituents were shown to lead to a rotational barrier higher than 10 kcal/mol. Hence, hindered internal rotation is suggested to cause one pyrrole conformer to be substantially overpopulated. This in turn has a major effect on π-facial selectivity of $^1O_2$, thereby favoring one endoperoxide over the other and leading to the diastereoselective synthesis of *trans*-pyrrolooxazolones. The importance of hindered internal rotors, for an accurate calculation of the frequency factors of a chemical reaction, has already been mentioned in the literature many times; however, in this work hindered internal rotors also seem to dictate the diastereoselective outcome of the reaction.

Introduction

Chiral nonracemic bicyclic lactams are extremely useful and versatile building blocks for the total synthesis of natural products and can be used as precursors and templates in a wide range of asymmetric synthesis[1,2] (Scheme 1).

Bicyclic lactams, with quaternary stereocenters, are valuable intermediates for many bioactive compounds.[3] Although, synthetic routes leading to cis-bicyclic lactams have been previously reported,[3b] the synthesis of trans isomers of these compounds is relatively new.[4]

Recent studies on the photooxygenation of homochiral *N*-(hydroxyalkyl)-2-methylpyrroles with $^1O_2$ furnished *trans*-pyrrolooxazolones in high diastereoselectivity.[4] The photooxygenation of the homochiral (*S*)-2-(2-methyl-1*H*-pyrrol-1-yl)-3-methylbutan-1-ol, (*S*)-**1**, led to a diastereomeric mixture of (*S*,*RS*)-3-isopropyl-7a-methyl-2,3-dihydropyrolo[2,1*b*][1,3]oxazol-5(7a*H*)-one, where the *trans*(*S*,*S*) and *cis*(*S*,*R*) products formed in a 5:1 isomeric ratio (Scheme 2). This study will focus on resolving the mechanistic aspects that have led to the diastereoselectivity in the synthesis of these bicyclic lactams.

Photooxygenation of nitrogen-containing heterocycles such as pyrroles,[5−7] imidazoles,[5,6,8] and other heterocycles[5,6,9] have been extensively studied. The reaction pattern and mechanism of photoinduced oxygenation reactions of N-substituted pyrroles have been explored both synthetically and mechanistically owing to their importance in photobiosynthesis and other biological processes.[7d−h] It is well-known that reactions of $^1O_2$ with heterocyclic compounds often give rise to a mixture of products depending on several factors such as the nature of the substrate and the functional groups in the immediate vicinity of the newly formed peroxide intermediates.[5a,10]

SCHEME 1: Bicyclic Lactams as Precursors in Various Synthetic Routes

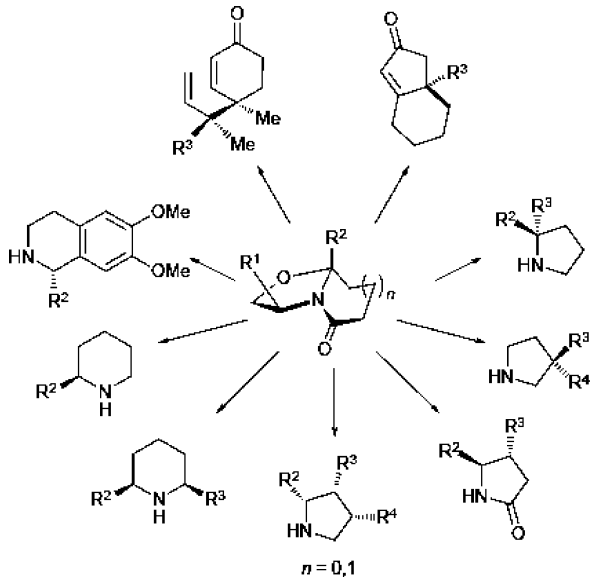

Singlet oxygen is known to give three major types of reactions, "ene" reactions with alkenes having allylic hydrogens to give allylic hydroperoxides,[11] [2 + 2] cyloadditions with

* To whom correspondence should be addressed. E-mail: aviye@boun.edu.tr.
[†] Bogazici University.
[‡] Middle East Technical University.

10.1021/jp071608y CCC: $37.00
Published on Web 06/13/2007

SCHEME 2: Chiral Bicyclic Lactams through Photooxygenation of (*S*)-*N*-(Hydroxyalkyl)-2-methylpyrroles with Singlet Oxygen[4]

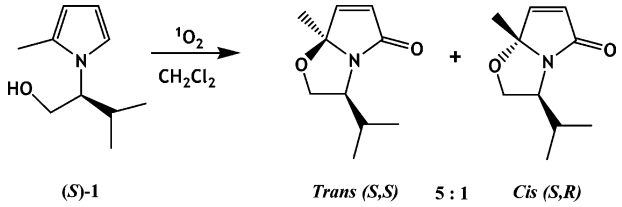

SCHEME 3: Diene: (*S*)-*N*-(Hydroxyalkyl)-Substituted 2-Methylpyrrole

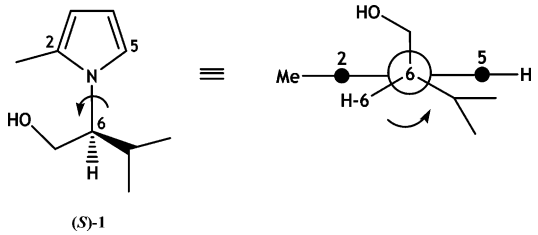

activated alkenes to give dioxetanes,[12] and [4 + 2] Diels−Alder cycloadditions with dienes to give endoperoxides.[13] The mechanisms of these reactions have received significant attention throughout the years.[14] Consequently, in this study, cycloaddition of $^1O_2$ to a homochiral N-substituted 2-methylpyrrole and subsequent reactions leading to a *trans*-pyrrolooxazolone will be investigated.

Singlet oxygen has been referred to as a superdienophile,[15] and the course of its cycloaddition is known to be highly sensitive to the diene's structure.[16] Adam et al. have extensively studied the π-facial selective attack of singlet oxygen toward cyclic dienes and have stated that stereocontrol for $^1O_2$ attack is a function of steric and electronic interactions; π-facial selectivity of $^1O_2$ can be *efficiently controlled by strategically placed substituents* at stereogenic sites in combination with strain-controlled conformational preferences.[16d] Substituents such as hydroxyl groups were shown to be very efficient in directing facial attack,[16c] by forming H-bonds with the $^1O_2$. However, electronic interactions such as H-bonding are only favorable in the case of electron-poor dienes, such as aromatic species. In cases where the diene is electron-rich, such as cyclopentadienes, sterics rule facial selectivity. This was explained through the difference in the charge-transfer complexes that form prior to cycloaddition.[16d] In this study, however, cycloaddition of singlet oxygen to a pyrolle—an aromatic, electron-poor diene—is under investigation; therefore, electronic interactions such as the hydroxyl group directing effect are expected to govern facial selectivity.

This article will focus on the origin of diastereoselectivity in the synthesis of the *trans*-pyrrolooxazolone[4] (Scheme 2) and investigate the mechanism of this reaction using computational methods.

Computational Methodology

All gas-phase geometry optimizations were performed using the density functional theory[17] (DFT) at the UB3LYP/6-31+G** level,[18] where both diffuse and polarization functions are included on heavy atoms, since utilization of diffuse functions is especially necessary in the optimization of anionic systems[19] and polarization functions are added on hydrogen atoms to account for the presence of hydrogen bonds.[20] All stationary points were characterized by a frequency analysis from which thermal corrections were also attained. Local minima and first-order saddle points were identified by the number of imaginary vibrational frequencies. The intrinsic reaction coordinate[21] (IRC) approach, followed by full geometry optimization, was used to determine the species reached by each transition structure. Energy values for gas-phase optimizations listed throughout the discussion include thermal free energy corrections at 298 K and 1 atm, unless otherwise stated.

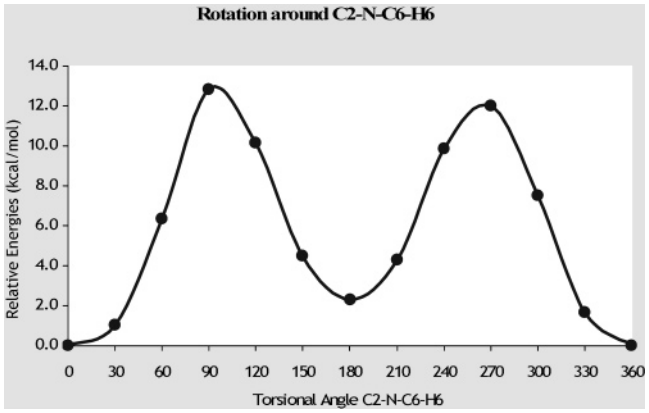

Figure 1. PES scan for pyrrole conformers (UB3LYP/6-31+G** in gas phase). Zero-point energies and free energy corrections are not included.

The effect of a polar environment was taken into account by use of the self-consistent reaction field (SCRF) theory, utilizing the integral equation formalism-polarizable continuum[22] (IEF-PCM) model in CH_2Cl_2 ($\epsilon = 8.93$) at the UB3LYP/6-31+G** level. Bondi radii[23] scaled by a factor of 1.2 were used for all solvent calculations. Energy values for solvent optimizations include thermal free energy corrections at 298 K and 1 atm as well as nonelectrostatic corrections.

A relaxed-potential energy surface (PES) scan,[24] in which geometry optimizations with dihedral constraints were carried out for each step, was performed on the pyrrole structure (*S*)-**1** in gas phase, to identify stationary points along the PES. Minima and rotational transition state geometries were further optimized in gas phase at the UB3LYP/6-31+G** level without any constraints. Full geometry optimizations on pyrrole (*S*)-**1** minima and rotational transition state structures were also performed in CH_2Cl_2 ($\epsilon = 8.93$) with IEF-PCM at the UB3LYP/6-31+G** level.

Preliminary analysis of the potential energy surfaces (PES) for the proposed mechanisms were carried out at a semiempirical level (PM3).[25] Further geometry optimizations were performed in gas phase at the UB3LYP/6-31+G** level. Geometries of stationary points were optimized without any constraints.

All energy values listed are in kcal/mol. All distances shown in the figures are in angstroms (Å). All gas phase and solvent calculations were carried out using the Gaussian 03 program package.[26] All structures shown in this study were optimized at the singlet state, and the stability of their wave functions was verified through calculations using the "stable" keyword.[27] $\langle S2 \rangle$ values for all optimized geometries were found to be zero, relieving concerns of spin contamination and the presence of biradical singlets.

Results and Discussion

In this study, we have explored the origin of selectivity in the diastereoselective synthesis of *trans*-pyrrolooxazolones via photooxidation of a homochiral N-substituted 2-methylpyrrole with $^1O_2$ (Scheme 2).[4] For this purpose, we have initially

SCHEME 4: Newman Projections of the Counterclockwise Rotation along the C2−N−C6−H6 Torsional Angle

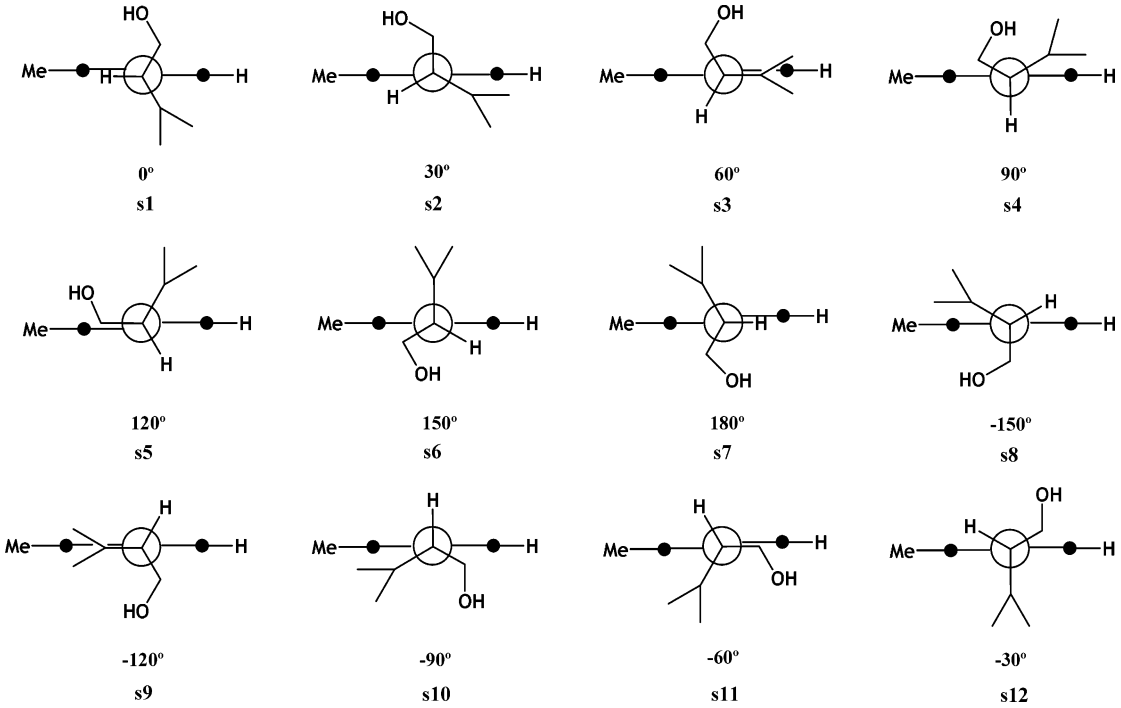

investigated the relative stabilities of (*S*)-**1**'s conformers, to rationalize the π-facial selectivity in the cycloaddition of singlet oxygen to the pyrrole ring. Second, we have proposed and modeled two reaction mechanisms—stepwise and concerted—starting from the Diels−Alder adducts to the bicyclic systems, to analyze the reaction barriers leading to the products and account for the experimentally observed product distribution.

Relative Stabilities of Pyrrole Conformers. As previously mentioned, Adam et al. have well-established the directing effect of hydroxyl substituents in Diels−Alder reactions involving $^1O_2$ and aromatic species.[16] Therefore, the conformational preference of the pyrrole's *N*-(hydroxyalkyl) substituent, particularly the position of the hydroxyl group with respect to the ring, will play a crucial role in the facial selectivity of the dienophile.

A thorough conformational search has been conducted on the (*S*)-*N*-(hydroxyalkyl)-2-methylpyrrole (Scheme 3). Given that the position of the hydroxyl group with respect to the ring is essential, a *relaxed*-potential energy surface (PES) scan has been performed for the counterclockwise rotation around the C2−N−C6−H6 dihedral angle. Constraints were applied *only* on this dihedral angle, and geometry optimizations were performed for each step. Energies of rotational conformers were calculated with 30° increments, in an effort to deduce the most stable conformers and the most favorable position of the hydroxyl group.

Newman projections of the above-mentioned rotation are shown in Scheme 4. The two main unfavorable steric interactions are among the methyl group on C-2 of the pyrrole ring and the −OH and isopropyl groups on the N-substituent.

Relative energies (UB3LYP/6-31+G** in gas phase) of all rotational conformers in the PES scan are depicted in Figure 1. Although the increment used in this PES scan is rather large, the smoothness of the resulting potential energy surface confirms its adequacy. This scan shows two minima at 0° (**s1**) and 180° (**s7**) and two maxima at 90° (**s4**) and −90° (**s10**). These four conformers were further optimized in both gas phase and solvent ($\epsilon = 8.93$) at the UB3LYP/6-31+G** level without constraints; herein they will be referred to as **min1**, **max1**, **min2**, and **max2**, respectively. Relative free energies of these conformers show a similar trend in gas phase and solvent (Table 1). Full geometry optimizations and frequency calculations indicate that **min1** is the global minimum, **min2** is a local minimum, and **max1** and **max2** are rotational transition states that connect these two minima. The barrier of rotation from either side is quite high (more than 10 kcal/mol); therefore, rotation around this bond is clearly largely hindered.

TABLE 1: Relative Free Energies for Fully Optimized Stationary Points on PES Scan with Zero-Point Energies and Free Energy Corrections Included

		relative energies	
conformer	dihedral angle C2−N−C6−H6	UB3LYP/6-31+G** ($\epsilon = 0$)	UB3LYP/6-31+G** (SCFR = IEF-PCM; $\epsilon = 8.93$)
min1	−0.747	0.0	0.0
max1	91.048	14.6	11.9
min2	−176.828	2.1	1.2
max2	−92.289	16.3	14.5

The difference in energy between the rotational transition states, **max1** and **max2**, is mainly due to the extra steric strain between the side chain isopropyl group and the 2-methyl group in the case of **max2** (Figure 1).

Analysis of the fully optimized structures **min1** and **min2** indicates that the favorable electronic interaction between the hydroxyl group and the π-electron cloud of the pyrrole ring is the main reason for the stability of these two conformers (Figure 3). The energy difference between the two minima, **min1** and **min2**, is mostly due to the more pronounced steric interaction between the isopropyl and methyl groups in the case of **min2**. Additionally, as a result of this hindrance a slight tilt in the dihedral angle for **min2** is observed (Table 1), which in turn adversely effects the electronic interaction between the π-cloud and the −OH moiety. This can be observed in the slight difference in distances shown in Figure 2. These two factors account for the 1.2 kcal/mol (2.1 kcal/mol in gas phase) energy difference between the two minima in solvent.

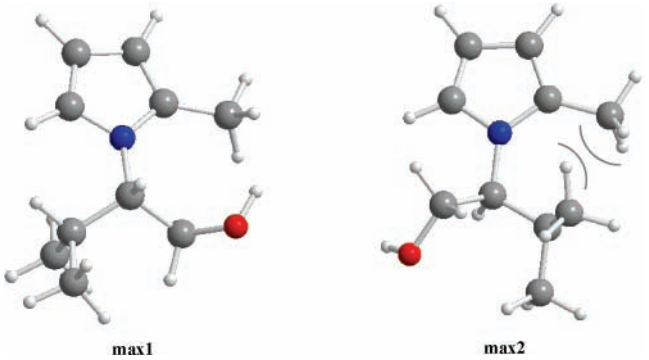

Figure 2. Optimized geometries (UB3LYP/6-31+G** IEF-PCM; $\epsilon = 8.93$) for the rotational transition states, **max1** and **max2**.

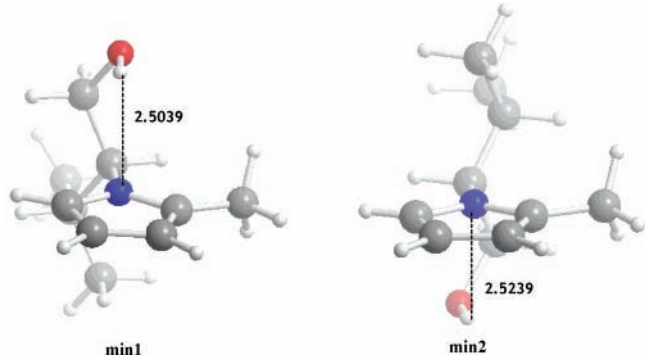

Figure 3. Optimized geometries (UB3LYP/6-31+G** IEF-PCM; $\epsilon = 8.93$) for minima, **min1** and **min2**.

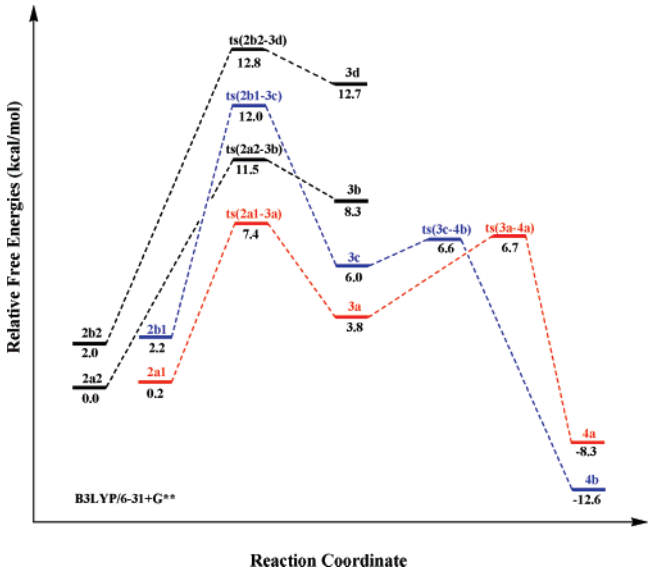

Figure 4. Potential free energy profile for the proposed reaction mechanism.

The hindered internal rotation between the two minima and the 1.2 kcal/mol energy difference between them suggest that the pyrrole ring will more likely assume conformation shown in **min1**. The probability of each conformer was calculated using the Boltzmann distribution. An energy difference of 1.2 kcal/mol corresponds to a 132/1000 ratio, which makes **min1** the predominant conformer of the pyrrole ring; however, the population of conformer **min2** is not insignificant. The ratio of **min1** to **min2** is approximately 23:3.

***π*-Facial Selectivity of Singlet Oxygen.** The analysis of the conformational preference of (*S*)-*N*-(hydroxyalkyl)-2-methylpyrrole was intended to shed light on the position of the hydroxyl group with respect to the pyrrole ring. As Adam et al. have previously stated, in the course of the cycloaddition reaction between singlet oxygen and the diene, $^1O_2$ initially forms a favorable electronic interaction with the hydroxyl group on the diene.[16] The directing effect of the hydroxyl group has been well-established with experiments. Therefore, the position of the hydroxyl group with respect to the pyrrole ring is of great interest in this study, since it will determine the ***π*-facial selectivity of** $^1O_2$.

SCHEME 5: Singlet Oxygen Addition to (*S*)-*N*-(Hydroxyalkyl)-2-methylpyrrole Forms Endoperoxides 2a,b

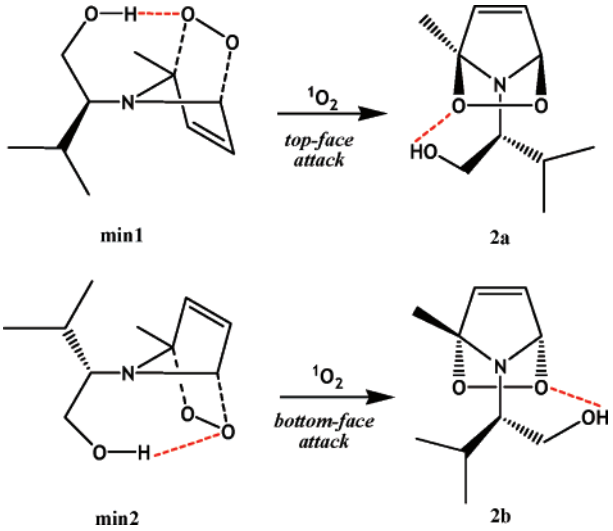

The cycloaddition of $^1O_2$ to a variety of acyclic, cyclic, and aromatic systems has been computationally studied.[14k−o] It is well-known that an endoperoxide intermediate forms upon cycloaddition of singlet oxygen to *cyclic*-diene systems.[14d] Singlet oxygen cycloaddition with similar aromatic dienes has shown clean endoperoxiation.[16d] Therefore, modeling the Diels−Alder step leading to the endoperoxide is not our main interest.

The (*S*)-*N*-(hydroxyalkyl)-2-methypyrrole undergoes photooxygenation with $^1O_2$ to form an endoperoxide ring (Scheme 5). The pyrrole ring can undergo a Diels−Alder fashion 1,4 addition of $^1O_2$ through both faces. Singlet oxygenaddition from the *top* face leads to the Diel−Alder adduct **2a**, whereas $^1O_2$ addition from the *bottom* face forms **2b**.

In the case of **min1**, the more abundant pyrrole conformer, the directing effect of the hydroxyl group will enhance facial attack of $^1O_2$ from the top face, hence lead to the formation of endoperoxide **2a**, whereas **min2**, the less prominent conformer, will promote attack from the bottom face leading to endoperoxide **2b**. Taking into account the distribution of pyrrole conformers previously discussed, endoperoxide **2a** is more likely to prevail. The positions of the isopropyl moieties in pyrrole conformers **min1** and **min2** (Figure 3) also indicate steric hindrance on the opposite face of the hydroxyl group in both cases, reaffirming that singlet oxygen addition will take place exclusively from the hydroxyl group's side and the percentage of singlet oxygen addition from the opposite face of the hydroxyl group can be considered insignificant.

Therefore, as Adam et al. have previously stated,[16] strain control and electronic interactions, such as the hydroxyl group directing effect, can be strategically combined to design a system where π-facial selectivity of $^1O_2$ can be efficiently controlled.

The fact that singlet oxygen's attack on different faces of the homochiral *N*-(hydroxyalkyl)-2-methylpyrrole leads to two different endoperoxides is noteworthy and will determine the

SCHEME 6: Proposed Stepwise Reaction Mechanism

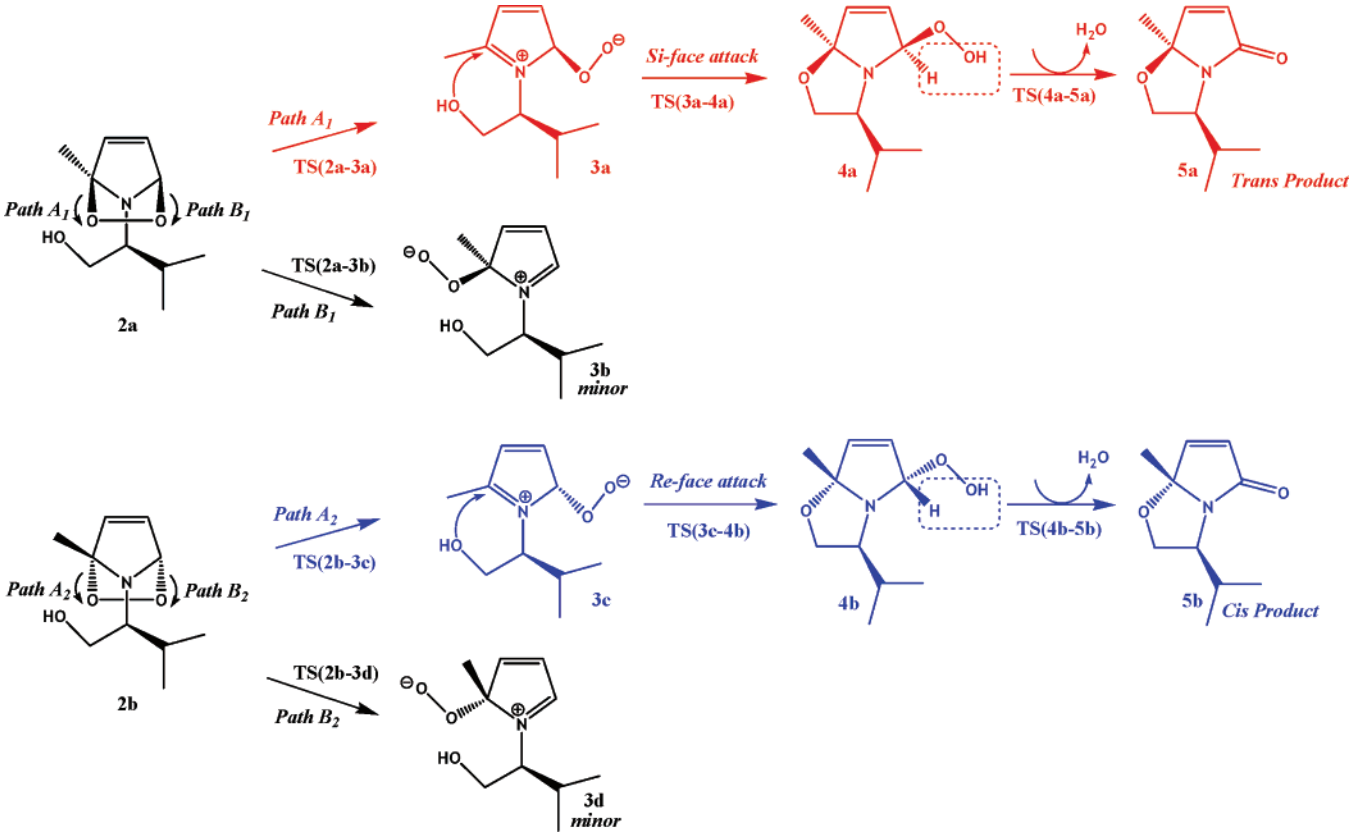

outcome of the reaction as discussed in the following section. The next part of the discussion will focus on the proposed reaction mechanisms and will illustrate how singlet oxygen's π-facial selective attack on the pyrrole ring results in diastereoselective synthesis of chiral bicyclic lactams.

Proposed Stepwise Reaction Mechanism. This section is dedicated to exploring a stepwise reaction mechanism that results in the diastereoselective synthesis of *cis*- and *trans*-pyrrolooxazolones. Scheme 6 shows the proposed stepwise reaction mechanism starting from endoperoxides (**2a**,**b**) leading to the bicyclic lactams. The free energy potential profile for the proposed stepwise reaction mechanism is depicted in Figure 4.

The first step (**2** → **3**) in the proposed mechanism is the heterolytic cleavage of the peroxide functionality from the ring carbon, which can occur either through path A_1 or path B_1 for **2a** and path A_2 or path B_2 for **2b**, where path A and path B are competing steps. Path A, in both cases, shows the cleavage of the peroxide ring from the carbon bearing the methyl group, whereas path B indicates cleavage from the opposite ring carbon.

The fact that the hydroxyl group can form H-bonds with either of the peroxide oxygen's leads to two conformers for each endoperoxide, namely conformers **2a1** and **2a2** for endoperoxide **2a** and conformers **2b1** and **2b2** for endoperoxide **2b** (Figure 5). Relative free energies (Figure 4) show 0.2 kcal/mol free energy difference between conformers of **2a** (**2a1** and **2a2)** and conformers of **2b** (**2b1** and **2b2**). The main structural difference between conformers of **2a** and conformers of **2b** is the unfavorable steric interaction of the isopropyl and methyl groups. These two groups are in close proximity in the **2b** conformers as opposed to their relative positions in the **2a** conformers (Figure 5). This steric interaction causes a free energy difference of 2 kcal/mol among endoperoxides **2a**,**b**, similar to the case of the pyrrole conformers discussed in the previous section.

Transition states **TS(2a1-3a)**, **TS(2a2-3b)**, **TS(2b1-3c),** and **TS(2b2-3d)** for path A_1, path B_1, path A_2, and path B_2 originate from endoperoxides **2a1**, **2a2**, **2b1**, and **2b2**, respectively. The negative charge that forms on the oxygen upon cleavage from the ring is stabilized via H-bonding with the side chain −OH group, in all four transition states. H-bond distances in these transition states, ranging from 1.58 to 1.62 Å, are quite short as a result of the charged oxygen involved (Figure 6).

The potential free energy profile (Figure 4) shows that the free energy of activation ($\Delta G^{\ddagger}$) leading to transition state **TS-(2a1-3a)** is 4.3 kcal/mol lower in energy than that for **TS(2a2-3b)**; similarly $\Delta G^{\ddagger}$ for **TS(2b1-3c)** is 1 kcal/mol lower than that for **TS(2b2-3d)**, indicating that **3a**,**c** are the two major products of this step. The free energy of activation for the formation of **3a** is 2.6 kcal/mol lower than that for **3c**. The main structural difference between these two transition states, **TS-(2a1-3a)** and **TS(2b1-3c)**, is once again the steric strain between the isopropyl and methyl groups, causing a repulsive interaction in the case of **TS(2b1-3c)**. This unfavorable interaction causes a slight change in the position of the −OH group, which in turn adversely affects the hydrogen-bonding distance, as shown in Figure 6. As a result, the negative charge on the peroxide group in **TS(2b1-3c)** is not as efficiently stabilized as in **TS-(2a1-3a)**, hence the energy difference.

Zwitterion **3a** is 4.5 kcal/mol more stable than **3b**; consequently, **3c** is 6.7 kcal/mol lower in energy than **3d**. Both zwitterions **3a**,**c** have methyl-substituted double bonds (Figure 7), which may account for their thermodynamic stability, as opposed to the less substituted double bonds that form in **3b**,**d**. Routes originating from **3b**,**d** do not give rise to the synthesis products shown in Scheme 2. Since the purpose of this study is

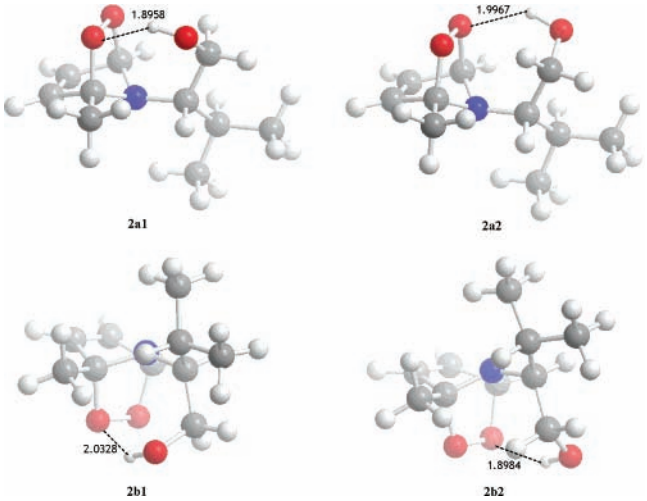

Figure 5. Optimized geometries (UB3LYP/6-31+G**) for endoperoxides **2a1**, **2a2**, **2b1**, and **2b2**.

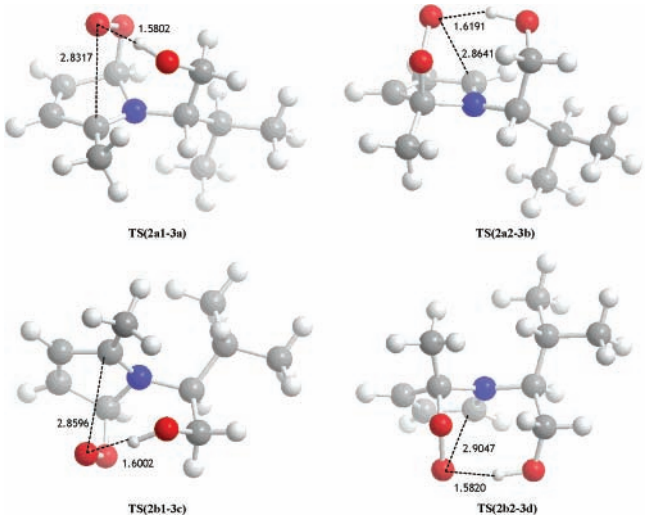

Figure 6. Optimized geometries (UB3LYP/6-31+G**) for transition states **TS(2a1-3a)**, **TS(2a2-3b)**, **TS(2b1-3c)**, and **TS(2b2-3d)**.

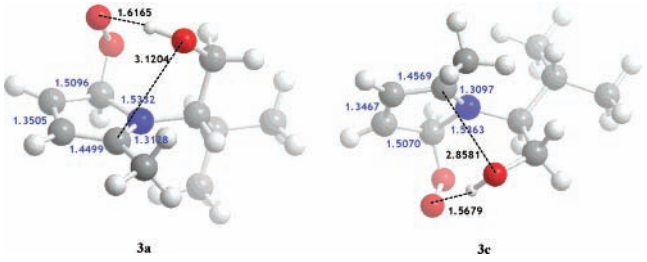

Figure 7. Optimized geometries (UB3LYP/6-31+G**) for zwitterionic intermediates, **3a**,**c**. Pyrrole ring atoms distances are given in blue.

to investigate pathways that lead to *cis*- and *trans*-pyrrolooxazolones, the fate of intermediates **3b**,**d** will not be further discussed. The mechanism leading to bicyclic lactams will be investigated via zwitterionic intermediates **3a**,**c**.

The next step is the ring closure (**3** → **4**), which leads to the *cis*- and *trans*-hydroperoxides (**4a**,**b**) as indicated in Scheme 5. As the side chain hydroxyl oxygen attacks the methyl-bearing carbon on the pyrrole ring, the hydroxyl hydrogen is transferred to the peroxide oxygen. Ring closure and proton transfer take place in a single step; hence, the hydroxyl group should attack from the face bearing the peroxide ion, in order for proton transfer to take place. Therefore, for **3a** side chain −OH attack on the pyrrole ring takes place from the *si*-face and for **3c** attack

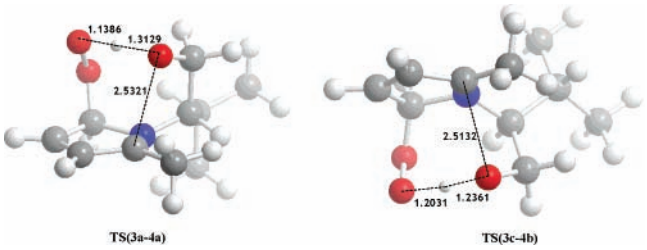

Figure 8. Optimized geometries (UB3LYP/6-31+G**) for ring closure transition states, **TS(3a-4a)** and **TS(3c-4b)**.

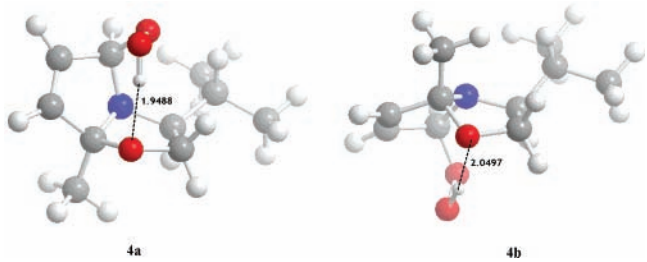

Figure 9. Optimized geometries (UB3LYP/6-31+G**) for the hydroperoxides, **4a**,**b**.

occurs from the *re*-face. Consequently, **3a** leads to the *trans*-hydroperoxide **4a** and **3c** gives the *cis*-hydroperoxide **4b**.

Transition state structures **TS(3a-4a)** and **TS(3c-4b)** represent the −OH attack from the *si*-face and the *re*-face, respectively (Figure 8). The critical distances given indicate that proton transfer takes place prior to ring closure; hence, this is an asynchronous concerted transition state. As a result *cis*- (**4a**) and a *trans*-hydroperoxides (**4b**) form (Figure 9).

Free energies of reaction (ΔG_{rxn}) show that the cis product (**4b**) is thermodynamically more stable than the trans product (**4a**); more specifically, **4b** is 4.3 kcal/mol more stable than **4a**, yet **4a** is the experimentally observed major product. All ΔG_{rxn}'s for step **3** → **4** are quite exothermic. Therefore, once the bicyclic system forms, it is highly unlikely that a reverse reaction will take place.

Although, $\Delta G^{\ddagger}$ for **4b** is 2.3 kcal/mol lower than that for **4a**, the free energy profile reveals that the first step (**2** → **3**), with the highest activation barriers, is the rate-determining step for the proposed stepwise reaction mechanism. Therefore, free energies of transition states **TS(2a1-3a)** and **TS(2b1-3c)** are essential in deducing the major pyrrolooxazolone that forms, cis versus trans. Relative free energies given in Figure 4 indicate that $\Delta G^{\ddagger}$ for **2a1** → **TS(2a1-3a)** is 7.2 kcal/mol, whereas $\Delta G^{\ddagger}$ for **2b1** → **TS(2b1-3c)** is 9.8 kcal/mol. Therefore, for the stepwise reaction mechanism proposed, *trans*-pyrrolooxazolone will be the major product. The results attained by the proposed stepwise reaction mechanism are consistent with experimental results and also reaffirm that the reaction is governed by kinetic rather than thermodynamic control.

The last step (**4** → **5**) in the proposed stepwise reaction mechanism (Scheme 6) involves the loss of a water molecule from the hydroperoxides (**4a**,**b**) to yield the pyrrolooxazolones (**5a**,**b**). This step is irrelevant with respect to the *stereoselectivity* in the synthesis of *cis*- and *trans*-pyrrolooxazolones; therefore, it will not be discussed herein. However, it should be noted that a concerted four-centered transition state with a high barrier is most likely involved in the early stages of the reaction. Nonetheless, as the reaction proceeds, water molecules that form can assist and catalyze this step.

It was previously suggested in this discussion that the relative stability of pyrrole conformers and π-facial selectivity of $^1O_2$

SCHEME 7: Proposed Concerted Reaction Mechanism

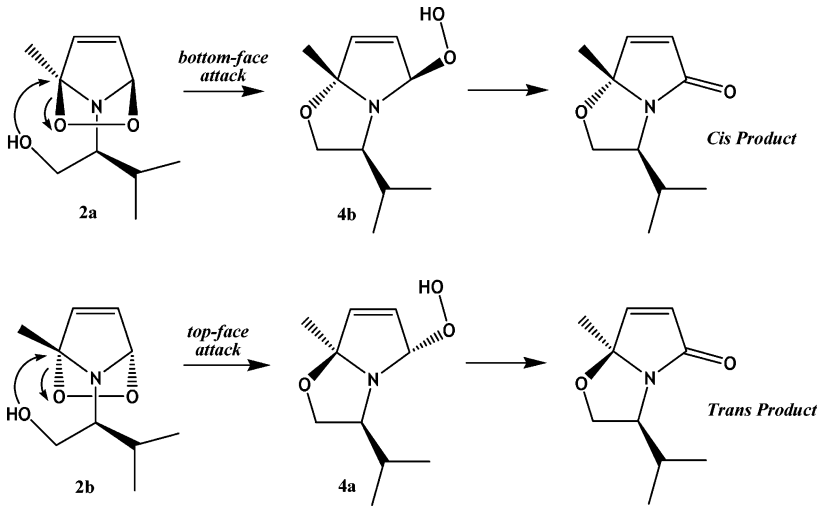

SCHEME 8: Origin of Diastereoselectivity in the Photooxygenation of (*R*)-*N*-(Hydroxyalkyl)-2-methylpyrroles with $^1O_2$: π-Facial Selective Attack of $^1O_2$ Induced by Hindered Internal Rotation

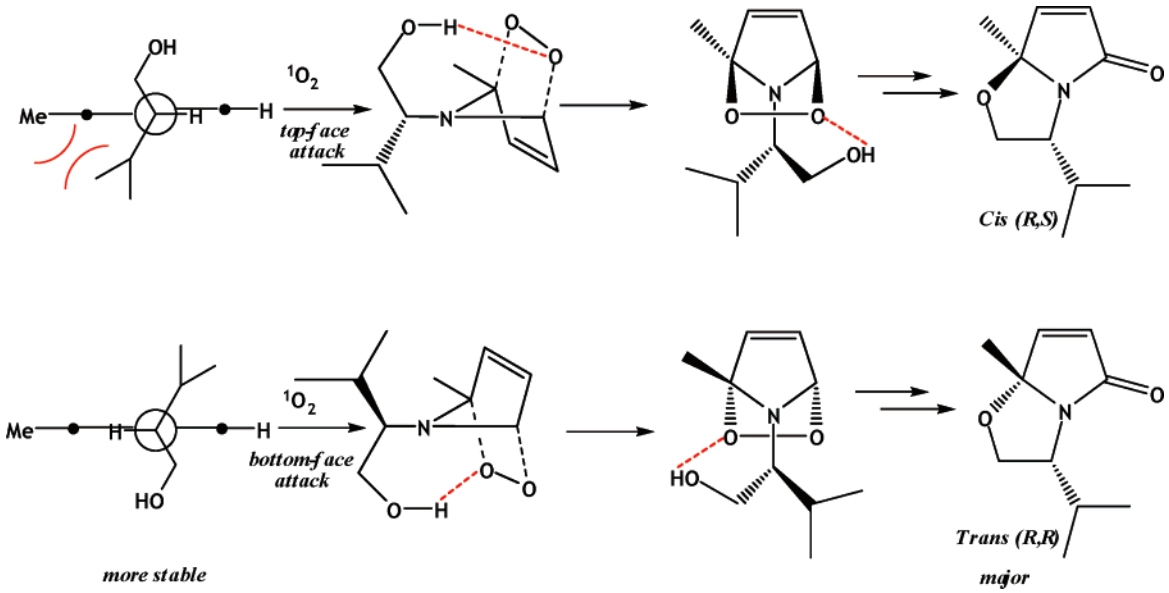

favors the formation of endoperoxide **2a** and the free energy of activation ($\Delta G^{\ddagger}$) for the steps that follow is also crucial in rationalizing the experimentally observed diastereoselectivity. In summary of the results deduced so far, the path originating from the major endoperoxide (**2a**) has a lower activation barrier in the rate-determining step of the proposed stepwise reaction and yields the thermodynamically less stable *trans*-pyrroloxazolone.

Although endoperoxide **2a** goes through a lower barrier than **2b** in the rate-determining step (**2** → **3**), it should be noted that these two pathways are not competitive. According to the proposed stepwise reaction mechanism, the concerted attack at step **3** → **4** ensures that only one diastereomer will form from each endoperoxide. The fact that the barrier leading to the trans product is lower than the one leading to the cis product does not effect the resulting product distribution. The fate of the reaction is determined once cycloaddition has taken place. Therefore, the hydroxyl group directing effect on π-facial selectivity of $^1O_2$ has played a major role in the diastereoselectivity observed in this reaction. However, the difference in populations of the two pyrrole conformers (**min1** and **min2**) as a result of hindered internal rotation on the pyrrole ring has led to a difference in product distribution in the cycloaddition step; **2a** is the *major* product whereas **2b** is the *minor* product. Hence, it can be concluded that the origin of diastereoselectivity in the synthesis of bicyclic lactams is the hindered internal rotation on the pyrrole ring.

The importance of hindered internal rotors, for an accurate calculation of the frequency factors of a chemical reaction, has already been extensively discussed in the literature;[28] however, in this work it also seems to dictate the diastereoselective outcome of the reaction. Similar directing effects where the reaction outcome must be attributed to a specific internal rotation, rather than thermodynamic stability, have been previously observed.[29]

The major deductions so far have shown that (a) the hindered internal rotation caused by steric hindrance of bulky groups on the pyrrole ring and (b) π-facial selectivity of $^1O_2$ caused by electronic interactions with the hydroxyl moiety on this ring have a combined effect on the outcome of this reaction. One can conclude that by efficiently utilizing these factors to strategically design a similar reaction, stereoselectivity can be induced and the thermodynamically less stable product can be attained in higher yield.

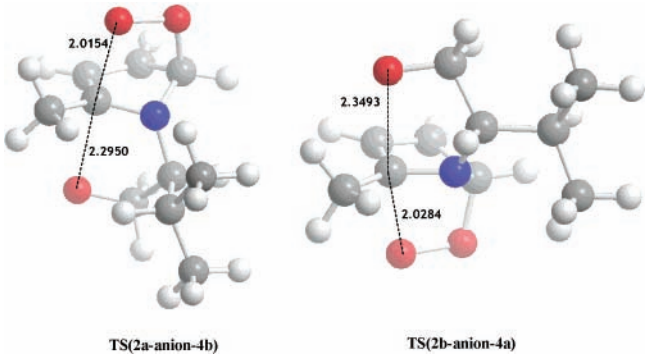

Figure 10. Optimized geometries (UB3LYP/6-31+G**) for the concerted intramolecular alcoholysis transition states, **TS(2a-anion-4b)** and **TS(2b-anion-4a)**.

Proposed Concerted Reaction Mechanism. In this section we will explore a concerted reaction mechanism for the diastereoselective synthesis of the *cis*- and *trans*-pyrrolooxazolones. The concerted reaction mechanism involves the simultaneous attack of the side chain −OH to the ring carbon bearing the methyl group and the cleavage of the peroxide oxygen from this carbon. It should be noted that a concerted attack can *only* occur from the opposite face from which the peroxide ring is accommodated due to an unfavorable steric and electronic interaction between the peroxide oxygen and the −OH. Nevertheless, the −OH group will still encounter steric hindrance from the methyl group during attack (Scheme 7). This is an S_N2 type reaction with intense steric strain. Such a concerted attack will also disable proton transfer to the peroxide group, as previously suggested in the proposed stepwise reaction mechanism, and reduce the nucleophilicity of the −OH moiety.

The proposed concerted reaction mechanism suggests that a concerted intramolecular alcoholysis on endoperoxide **2a** would produce *cis*-**4b**; on the other hand, *trans*-**4a** would form if the reaction goes through **2b**. The mechanism has been computationally explored; however, stationary points and transition state structures could not be located. The −OH functionality was not nucleophilic enough for ring closure. For this reaction to occur, the side chain −OH must be converted into a stronger nucleophile, such as an oxyanion. However, it should be noted that experimental reaction conditions do not facilitate deprotonation of the alcohol group. It would require strongly basic impurities to form these anions, since they are not well solvated in nonpolar solvents, such as dichloromethane. In fact, it is highly unlikely that the reaction medium is basic enough to deprotonate the alcohol group. On the other hand, intramolecular proton transfer would require the alcohol moiety to be on the same face with the peroxide group, which would disable a backside attack as suggested in the concerted reaction mechanism. Nevertheless, the concerted reaction mechanism was modeled with oxyanions of endoperoxides **2a**,**b** by assuming that deprotonation might somehow take place. The deprotonation step, however, has not been computationally investigated, since it is irrelevant to the selectivity that is being explored.

Figure 10 shows gas-phase-optimized (UB3LYP/6-31+G**) geometries of transition structures **TS(2a-anion-4b)** and **TS-(2b-anion-4a)**. The distance between the side chain oxyanion and the ring carbon in these transition states is approximately 2.3 Å, whereas the peroxide oxygen departing from the ring carbon is around 2.0 Å, indicating fairly synchronous transition states.

The free energy of activation leading to the cis product **4b** is 0.5 kcal/mol higher in energy than that for the trans product **4a**. However, the difference in $\Delta G^{\ddagger}$ is rather small for a legitimate comparison at the UB3LYP/6-31+G** level.

Contrary to experimental findings, if oxyanion formation were to somehow occur, considering endoperoxide **2a** is the major product of the cycloaddition, the *cis*-pyrrolooxazolone would have been the major product of this reaction. Therefore, the concerted reaction mechanism fails to explain the diastereoselectivity observed in this synthesis.

π-Facial Selective Attack of Singlet Oxygen to (*R*)-*N*-(Hydroxyalkyl)-2-methylpyrrole: An Intuitive Approach. In light of the results and discussions drawn for the singlet oxygen photooxygenation of (*S*)-*N*-(hydroxyalkyl)-2-methylpyrrole, (*S*)-**1**, it is worthwhile to take a look at the (*R*)-*N*-(hydroxyalkyl)-2-methylpyrrole. Experiments have shown that the photooxygenation of the (*R*)-2-(2-methyl-1*H*-pyrrol-1-yl)-3-methylbutan-1-ol, (*R*)-**1**, has likewise led to a diastereomeric mixture of (*R*,*RS*)-3-isopropyl-7a-methyl-2,3-dihydropyrolo[2,1*b*][1,3]oxazol-5(7a*H*)-one, where the *trans*(*R*,*R*) and *cis*(*R*,*S*) products formed in a 5:1 isomeric ratio.[4]

Briefly looking at the underlying reasons for this diastereoselectivity, we can again conclude that, among the two prospective minima for (*R*)-**1**, one has less steric hindrance and therefore is likely to be more stable (Scheme 8). This conformer will subsequently effect the outcome of this reaction by directing the singlet oxygen to the *bottom* face of the pyrrole ring. As a result one endoperoxide will form with greater yield and undergo a stepwise reaction to form the major product, *trans*(*R*,*R*)-pyrrolooxazolone. This reaffirms that the factors we have claimed to govern diastereoselectivity hold for the pyrrole's (*R*)-enantiomer.

Conclusion

In this study, we have attempted to elucidate the diastereoselectivity in the photooxygenation of homochiral *N*-(hydroxyalkyl)-2-methylpyrroles with singlet oxygen (Scheme 2). Although *cis*-pyrrolooxazolones are thermodynamically more stable, experimental results revealed *trans*-pyrrolooxazolones as the major product of this reaction.[4]

Calculations showed that the N-substituent on the pyrrole ring was large enough to induce hindered internal rotation, which in turn caused one conformer (**min1**) to be more populated. Diastereofacial attack of $^1O_2$, directed by the hydroxyl group on the pyrrole conformer, formed the major cycloaddition adduct, endoperoxide **2a**. Both a stepwise and concerted reaction mechanism was proposed and modeled for the reaction path from the endoperoxides to the bicyclic lactams. The proposed stepwise reaction mechanism was shown to form the *trans*-bicyclic lactam as the major product.

Hindered internal rotation is suggested to be the origin of diastereoselectivity in this study, since the reaction outcome is induced by a specific internal rotation, rather than thermodynamic stability. The hydroxyl group directing effect governing the π-facial selectivity of $^1O_2$ has also played a major role in the outcome of this reaction. It can be concluded that strategic use of these factors can benefit the design of similar reactions, whereby stereoselectivity can be induced to attain the thermodynamically less stable product in higher yield.

Acknowledgment. The computational resources used in this work were provided by the TUBITAK ULAKBIM High Performance Computing Center and by the Bogazici University Research Foundation (BAP). S.C. thanks Dr. Veronique van Speybroeck (Ghent University, Ghent, Belgium) for fruitful discussions. S.C. also acknowledges a TUBITAK National Ph.D. Scholarship.

Supporting Information Available: Cartesian coordinates for all optimized structures, energetics data, and complete ref 26. This material is available free of charge via the Internet at http://pubs.acs.org.

References and Notes

(1) Meyers, A. I.; Brengel, G. P. *J. Chem. Soc., Chem Commun.* **1997**, 1.

(2) (a) Romo, D.; Romine, J. L.; Midura, W.; Meyers, A. I. *Tetrahedron* **1990**, *46*, 4951. (b) Meyers, A. I.; Bienz, S. *J. Org. Chem.* **1990**, *55*, 791. (c) Brengel, G. P.; Meyers, A. I. *J. Org. Chem.* **1996**, *61*, 3230. (d) Romo, D.; Meyers, A. I. *Tetrahedron* **1991**, *47*, 9503. (e) Romo, D.; Meyers, A. I. *J. Org. Chem.* **1992**, *57*, 6265. (f) Meyers, A. I.; Westrum, L. J. *Tetrahedron Lett.* **1993**, *34*, 7701. (g) Meyers, A. I. In *Stereocontrolled Organic Synthesis*; Trost, B. M., Ed.; Blackwell Scientific Publications: Cambridge, MA, 1994; pp 145. (h) Es-Sayed, M.; Devine, P.; Burgess, L. E.; Meijere, A.; Meyers, A. I. *J. Chem. Soc., Chem. Commun.* **1995**, 141. (i) Andres, C. J.; Spetseris, N.; Norton, J. R.; Meyers, A. I. *Tetrahedron Lett.* **1995**, *36*, 1613. (j) Schwarz, J. B.; Meyers, A. I. *J. Org. Chem.* **1995**, *60*, 6511. (k) Wunsch, T.; Meyers, A. I. *J. Org. Chem.* **1990**, *55*, 4233.

(3) (a) Meyers, A. I.; Harre, M.; Garland, R. *J. Am. Chem. Soc.* **1984**, *106*, 1146. (b) Meyers, A. I.; Lefker, B. A.; Sowin, T. J.; Westrum, L. J. *J. Org. Chem.* **1989**, *54*, 4243.

(4) Aydogan, F.; Demir, A. S. *Tetrahedron: Asymmetry* **2004**, *15*, 259.

(5) (a) George, M. V.; Bhat, V. *Chem. Rev.* **1979**, *79*, 447. (b) Matsuura, T. *Tetrahedron* **1977**, *33*, 2869.

(6) Wasserman, H. H., Murray, R. W., Eds. S*inglet Oxygen*; Academic Press: New York, 1979; p 447.

(7) (a) Wasserman, H. H.; De Simone, R. W.; Boger, D. L.; Baldino, C. M. *J. Am. Chem. Soc.* **1993**, *115*, 8457. (b) Wasserman, H. H.; Frechette, R.; Rotello, V. M. *Tetrahedron Lett.* **1991**, *32*, 7571. (c) Li, H.-Y.; Drummond, S.; De Lucca, I.; Boswell, G. A. *Tetrahedron* **1996**, *52*, 11153. (d) Wasserman, H. H.; Petersen, A. K.; Xia, M.; Wang, J. *Tetrahedron Lett.* **1999**, *40*, 7587. (e) Wasserman, H. H.; Rotllo, V. M.; Frechette, R.; DeSimone, R. W.; Yoo, J. U.; Baldino, C. M. *Tetrahedron* **1997**, *53*, 8731. (f) Wasserman, H. H.; Xia, M.; Wang, J.; Petersen, A. K.; Jorgensen, M. *Tetrahedron Lett.* **1999**, *40*, 6145. (g) Boger, D. L.; Baldino, C. M. *J. Am. Chem. Soc.* **1993**, *115*, 11418. (h) Muratake, H.; Abe, I.; Natsume, M. *Tetrahedron Lett.* **1994**, *35*, 2573.

(8) (a) Kang, P.; Foote, C. S. *J. Am. Chem. Soc.* **2002**, *124*, 9629. (b) Kang, P.; Foote, C. S. *J. Am. Chem. Soc.* **2002**, *124*, 4865. (c) Sheu, C.; Kang, P.; Khan, S.; Foote, C. S. *J. Am. Chem. Soc.* **2002**, *124*, 3905. (d) Chawla, H. M.; Pathak, M. *Tetrahedron* **1990**, *46*, 1331.

(9) Li, Y.; Hu, H. Y.; Ye, J. P.; Fun, H. K.; Hu, H. W.; Xu, J. H. *J. Org. Chem.* **2004**, *69*, 2332.

(10) Lightner, D. A.; Bisacchi, G. S.; Norris, R. D. *J. Am. Chem. Soc.* **1976**, *98*, 802.

(11) (a) Adam, W.; Nestler, B. *J. Am. Chem. Soc.* **1992**, *114*, 6550. (b) Linker, T.; Frirhlich, L. *J. Am. Chem. Soc.* **1995**, *117*, 2694. (c) Houk, K. N.; Williams, J. C., Jr.; Mitchell, P. A.; Yamaguchi, K. *J. Am. Chem. Soc.* **1981**, *103*, 949. (d) Adam, W.; Peters, K.; Peters, E. M.; Schambony, S. B. *J. Am. Chem. Soc.* **2000**, *122*, 7610. (e) Adam, W.; Bottke, N.; Engels, B.; Krebs, O. *J. Am. Chem. Soc.* **2001**, *123*, 5542. (f) Adam, W.; Renze, J.; Wirth, T. *J. Org. Chem.* **1998**, *63*, 226.

(12) (a) Greer, A.; Vassilikogiannakis, G.; Lee, K. C.; Koffas, T. S.; Nahm, K.; Foote, C. S. *J. Org. Chem.* **2000**, *65*, 6876. (b) Maranzana, A.; Ghigo, G.; Tanachini, G. *J. Am. Chem. Soc.* **2000**, *122*, 1414. (c) Adam, W.; Saha-Moller, C. R.; Schambony, S. B. *J. Am. Chem. Soc.* **1999**, *121*, 1834. (d) Matsumoto, M.; Kobayashi, H.; Matsubara, J.; Watanabe, N.; Yamashita, S.; Oguma, D.; Kitano, Y.; Ikawa, H. *Tetrahedron Lett.* **1996**, *37*, 397.

(13) (a) Aubry, J. M.; Mandard-Cazin, B.; Rougees, M.; Bensasson, R. V. *J. Am. Chem. Soc.* **1995**, *117*, 9159. (b) Clennan, E. L.; Mehrsheikh-Mohammadi, M. E. *J. Am. Chem. Soc.* **1984**, *106*, 7112. (c) Clennan, E. L.; Mehrsheikh-Mohammadi, M. E. *J. Am. Chem. Soc.* **1983**, *105*, 5932. (d) Clennan, E. L.; Mehrsheikh-Mohammadi, M. E. *J. Org. Chem.* **1984**, *49*, 1321. (e) Adam, W.; Guthlein, M.; Peters, E. M.; Peters, K.; Wirth, T. *J. Am. Chem. Soc.* **1998**, *120*, 4091. (f) Chien, S. H.; Cheng, M. F.; Lau, K. C.; Li, W. K. *J. Phys. Chem. A* **2005**, *109*, 7509. (g) Pierlot, C.; Poprawski, J.; Marko, J.; Aubry, J. M. *Tetrahedron Lett.* **2000**, *41*, 5063. (h) Brecht, R.; Buttner, F.; Bohm, M.; Seitz, G.; Frenzen, G.; Pilz, A.; Massa, W. *J. Org. Chem.* **2001**, *66*, 2911. (i) Davis, K. M.; Carpenter, B. K. *J. Org. Chem.* **1996**, *61*, 4617.

(14) (a) Scharf, H.; Esser, P. *Angew. Chem., Int. Ed. Engl.* **1994**, *33*, 2009. (b) Poon, T.; Sivaguru, J.; Franz, R.; Jockusch, S.; Martinez, C.; Washington, I.; Adam, W.; Inoue, Y.; Turro, N. J. *J. Am. Chem. Soc.* **2004**, *126*, 10498. (c) Lissi, E. A.; Encinas, M. V.; Lemp, T.; Rubiot, M. A. *Chem. Rev.* **1993**, *93*, 699. (d) Balci, M. *Chem. Rev.* **1981**, *81*, 91. (e) Frimer, A. A. *Chem. Rev.* **1979**, *79*, 359. (f) Frimer, A. A. In *Singlet Oxygen*; Frimer, A. A., Ed.; CRC: Boca Raton, FL, 1985. (g) Clennan, E. L. *Tetrahedron* **2000**, *56*, 9151. (h) Manring, L. E.; Foote, C. S. *J. Am. Chem. Soc.* **1983**, *105*, 471. (i) Kearns, D. R.; Hasty, N. M. *J. Am. Chem. Soc.* **1973**, *95*, 3381. (j) Kearns, D. R. *J. Am. Chem. Soc.* **1969**, *91*, 6555. (k) Bobrowski, M.; Liwo, A.; Oldziej, S.; Jeziorek, D.; Ossowski, T. *J. Am. Chem. Soc.* **2000**, *122*, 8112. (l) Sevin, F.; McKee, M. L. *J. Am. Chem. Soc.* **2001**, *123*, 4591. (m) Leach, A. G.; Houk, K. N. *Chem. Commun.* **2002**, 1243. (n) Yoshioka, Y.; Tsunesada, T.; Yamaguchi, K.; Saito, I. *Int. J. Quantum Chem.* **1997**, *65*, 787. (o) Liwo, A.; Dyl, D.; Jeziorek, D.; Nowacka, M.; Ossowski, T.; Woznicki, W. *J. Comput. Chem.* **1997**, *18*, 1668.

(15) Hathaway, S. J.; Paquette, L. A. *Tetrahedron* **1985**, *41*, 2037.

(16) (a) Adam, W.; Prein, M. *Tetrahedron* **1995**, *51*, 12583. (b) Adam, W.; Prein, M. *Tetrahedron Lett.* **1994**, *35*, 4331. (c) Adam, W.; Prein, M. *J. Am. Chem. Soc.* **1993**, *115*, 3766. (d) Adam, W.; Prein, M. *Acc. Chem. Res.* **1996**, *29*, 275. (e) Adam, W.; Peters, K.; Peters, E. M.; Rein, M.; Schneringt, H. G. *J. Am. Chem. Soc.* **1995**, *117*, 6686.

(17) (a) Parr, R. G.; Yang W. *Density-functional theory of atoms and molecules*; Oxford Univ. Press: Oxford, U.K., 1989. (b) Hohenberg, P.; Kohn, W. *Phys. Rev.* **1964**, *136*, B 864. (c) Kohn, W.; Sham, L. *J. Phys. Rev.* **1965**, A1133.

(18) (a) Becke, A. D. *J. Chem. Phys.* **1993**, *98*, 5648−5652. (b) Lee, C.; Yang, W.; Parr, R. G. *Phys. Rev.* **1988**, *B37*, 785. (c) Madura, J.; Jorgensen, W. L. *J. Am. Chem. Soc.* **1986**, *108*, 2517.

(19) Barbour, J. B.; Karty, J. M. *J. Org. Chem.* **2004**, *69*, 648.

(20) Chung, G.; Kwon, O.; Kwon, Y. *J. Phys. Chem. A* **1997**, *101*, 4628.

(21) (a) Gonzalez, C.; Schlegel, H. B. *J. Chem. Phys.* **1989**, *90*, 2154. (b) Gonzalez, C.; Schlegel, H. B. *J. Phys. Chem.* **1990**, *94*, 5523.

(22) (a) Tomasi, J.; Mennucci, B.; Cancès, E. *J. Mol. Struct. (THEOCHEM)* **1999**, *464*, 211. (b) Cancès, M. T.; Mennucci, B.; Tomasi, J. *J. Chem. Phys.* **1997**, *107*, 3032. (c) Mennucci, B. Tomasi, J. *J. Chem. Phys.* **1997**, *106*, 5151. (d) Mennucci, B.; Cancès, E.; Tomasi, J. *J. Phys. Chem. B* **1997**, *101*, 10506.

(23) Bondi, A. *J. Phys. Chem.* **1964**, *68*, 441.

(24) Foresman, J. B.; Frisch, A. E. *Exploring Chemistry with Electronic Structure Methods*, 2nd ed.; Gaussian, Inc.: Pittsburgh, PA, 1996.

(25) (a) Stewart, J. J. P. *J. Comput. Chem.* **1989**, *10*, 221. (b) Stewart, J. J. P. *J. Comput. Chem.* **1989**, *10*, 209.

(26) Frisch, M. J.; et al. *Gaussian 03*, revision B.05; Gaussian, Inc.: Wallingford, CT, 2004.

(27) (a) Seeger, R.; Pople, J. A. *J. Chem. Phys.* **1977**, 66. (b) Bauernschmitt R.; Ahlrichs, R. *J. Chem. Phys.* **1996**, *104*, 9047.

(28) (a) Heuts, J. P. A.; Gilbert, R. G.; Radom, L. *Macromolecules* **1995**, *28*, 8771. (b) Van Speybroeck, V.; Van Neck, D.; Waroquier, M.; Wauters, S.; Saeys, M.; Marin, G. B. *J. Phys. Chem. A* **2000**, *104*, 10939.

(29) Van Speybroeck, V.; Moonen, K.; Hemelsoet, K.; Stevens, C. V.; Waroquier, M. *J. Am. Chem. Soc.* **2006**, *128*, 8468.